

Constituent quarks and systematic errors in mid-rapidity charged multiplicity $dN_{\text{ch}}/d\eta$ distributions.

M. J. Tannenbaum *

*Physics Department, 510c, Brookhaven National Laboratory,
Upton, NY 11973-5000, USA
mjt@bnl.gov*

Published December 29, 2017

Abstract

Centrality definition in A+A collisions at colliders such as RHIC and LHC suffers from a correlated systematic uncertainty caused by the efficiency of detecting a p+p collision ($50 \pm 5\%$ for PHENIX at RHIC). In A+A collisions where centrality is measured by the number of nucleon collisions, N_{coll} , or the number of nucleon participants, N_{part} , or the number of constituent quark participants, N_{qp} , the error in the efficiency of the primary interaction trigger (Beam-Beam Counters) for a p+p collision leads to a correlated systematic uncertainty in N_{part} , N_{coll} or N_{qp} which reduces binomially as the A+A collisions become more central. If this is not correctly accounted for in projections of A+A to p+p collisions, then mistaken conclusions can result. A recent example is presented in whether the mid-rapidity charged multiplicity per constituent quark participant $(dN_{\text{ch}}/d\eta)/N_{\text{qp}}$ in Au+Au at RHIC was the same as the value in p+p collisions.

1 From Nucleon Participants (Wounded Nucleons) to Constituent Quark Participants accounting for systematic errors

Measurements of charged particle multiplicity N_{ch} and transverse energy E_T distributions in A+A collisions in the c.m. energy range $10 \leq \sqrt{s_{NN}} \leq 20$ GeV found the surprising result that the average charged particle multiplicity $\langle N_{\text{ch}} \rangle$ in hadron+nucleus (h+A) collisions was not simply proportional to the number of collisions (absorption-mean-free-paths), N_{coll} , but increased much more slowly, proportional to the number of nucleon participants, N_{part} .^{1,2} This is known as the Wounded Nucleon Model (WNM).³

However, the first measurements of $dN_{\text{ch}}/d\eta$ (Ref. 4) and $dE_T/d\eta$ (Ref. 5) as a function of centrality at $\sqrt{s_{NN}} = 130$ GeV at RHIC did not depend linearly on N_{part} but had a non-linear increase of $dN_{\text{ch}}/d\eta$ and $dE_T/d\eta$ with increasing N_{part} illustrated by the fact that $(dE_T/d\eta)/N_{\text{part}}$ in Fig. 1(a) is not constant but increases with N_{part} . The comparison to the WA98 measurement⁶ in Pb+Pb at $\sqrt{s_{NN}} = 17.2$ GeV is also interesting because it is

*Research supported by U. S. Department of Energy, DE-SC0012704.

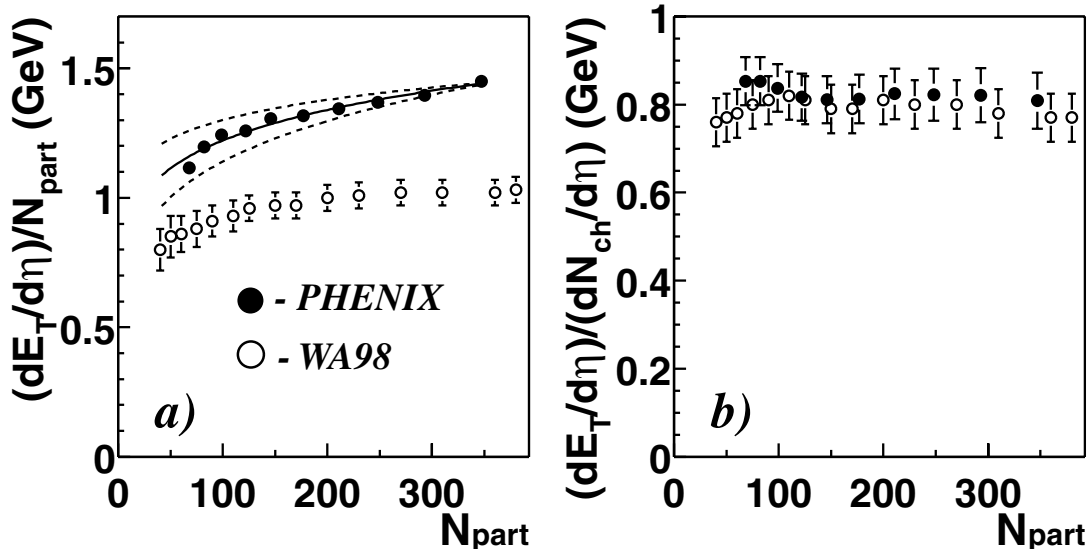


Figure 1: a)(left) PHENIX⁵ transverse energy density per participant $(dE_T/d\eta)/N_{\text{part}}$ for Au+Au at $\sqrt{s_{NN}} = 130$ GeV as a function of N_{part} , compared to the data⁶ of WA98 for Pb+Pb collisions at $\sqrt{s_{NN}} = 17.2$ GeV. b) (right) ratio of $(dE_T/d\eta)/(dN_{\text{ch}}/d\eta)$.

basically constant for $N_{\text{part}} > 200$, indicating that the WNM works at $\sqrt{s_{NN}} = 17.2$ GeV in this region.

The relevant point about the PHENIX $(dE_T/d\eta)/N_{\text{part}}$ measurement for the present discussion (Fig. 1a) is that the statistical errors are negligible. The dashed lines represent the $\pm 1\sigma$ effect of the correlated systematic error. In PHENIX we call these Type B correlated systematic errors⁷—all the points move together by the same fraction of the systematic error at each point. For instance, if all the points moved up to the dashed curve, which is $+1.0$ times the systematic error at each point, this will add only $1.0^2 = +1.0$ to the value of χ^2 of a fit with all 10 points moved. The fit⁷ takes account of the statistical (σ_i) and correlated systematic (σ_{b_i}) errors for each data point with value y_i :

$$\chi^2 = \left[\sum_{i=1}^n \frac{(y_i + \epsilon_b \sigma_{b_i} - y_i^{\text{fit}})^2}{\tilde{\sigma}_i^2} \right] + \epsilon_b^2 \quad , \quad (1)$$

where $\tilde{\sigma}_i$ scales the statistical error σ_i by the shift in y_i such that the fractional error remains unchanged: $\tilde{\sigma}_i = \sigma_i (1 + \epsilon_b \sigma_{b_i}/y_i)$, where ϵ_b is to be fit.

1.1 The PHENIX2014 N_{qp} model⁸

The massive constituent quarks,^{9–11} which form mesons and nucleons (e.g. a proton= uud), are relevant for static properties and soft physics such as multiplicity and E_T distributions composed predominantly of particles with $p_T \lesssim 1.4$ GeV/c in p+p collisions. Constituent quarks are complex objects or quasiparticles¹² made of the massless partons (valence quarks, gluons and sea quarks) of DIS¹³ such that the valence quarks acquire masses $\approx 1/3$ the nucleon mass with radii ≈ 0.3 fm when bound in the nucleon. With finer resolution (Fig. 2) one can see inside the bag to resolve the massless partons which can scatter at large angles according to QCD. At RHIC, hard-scattering starts to be visible as a power law above



Figure 2: Sketch of constituent quarks in a proton (diameter 1.6 fm) with improving resolution: (left) ≈ 0.5 fm, (center) ≈ 0.1 fm, (right) < 0.07 fm, massless quarks, sea quarks and gluons clearly resolved

soft (exponential) particle production at mid-rapidity only for $p_T > 1.4$ GeV/c,¹⁴ where $Q^2 = 2p_T^2 = 4$ (GeV/c)² which corresponds to a distance scale (resolution) < 0.1 fm.

The first 3 calculations which showed that N_{ch} was linearly proportional to¹⁵⁻¹⁷ N_{qp} only studied Au+Au collisions and simply generated three times the number of nucleons according to the Au radial distribution, Eq. 2,

$$\frac{d^3\mathcal{P}}{d^3r} = \frac{d^3\mathcal{P}}{r^2 dr \sin\theta d\theta d\phi} = \rho_N(r) = \frac{\rho_0}{1 + \exp(\frac{r-c}{a_0})} \quad (2)$$

with $c = \{1.18A^{1/3} - 0.48\}$ fm and the diffusivity $a_0 = 0.545$ fm for Au, called them constituent quarks and let them interact with the conventional constituent $q+q$ cross section $\sigma_{q+q}^{\text{inel}} = \sigma_{N+N}^{\text{inel}}/9$, e.g $\sigma_{q+q}^{\text{inel}} = 41\text{mb}/9 = 4.56$ mb at $\sqrt{s_{NN}} = 130$ GeV.¹⁵

The PHENIX2014 method⁸ was different from these N_{qp} calculations in that it used the E_T distribution measured in p+p collisions to derive the E_T distribution of a constituent quark to use as the basis of the calculations of the d+Au and Au+Au distributions. The PHENIX2014 calculation⁸ is a Monte Carlo which starts by generating the positions of the nucleons in each nucleus of an A+B collision, or simply the two nucleons in a p+p collision, by the standard method. Then the spatial positions of the three quarks are generated around the position of each nucleon using the proton charge distribution corresponding to the Fourier transform of the form factor of the proton:^{18,19}

$$\rho^{\text{proton}}(r) = \rho_0^{\text{proton}} \times \exp(-ar), \quad (3)$$

where $a = \sqrt{12}/r_m = 4.27$ fm⁻¹ and $r_m = 0.81$ fm is the r.m.s radius of the proton weighted according to charge¹⁸

$$r_m = \int_0^\infty r^2 \times 4\pi r^2 \rho^{\text{proton}}(r) dr \quad . \quad (4)$$

The corresponding proton form factor is the Hofstadter dipole fit²⁰ now known as the standard dipole:²¹

$$G_E(Q^2) = G_M(Q^2)/\mu = \frac{1}{(1 + \frac{Q^2}{0.71\text{GeV}^2})^2} \quad (5)$$

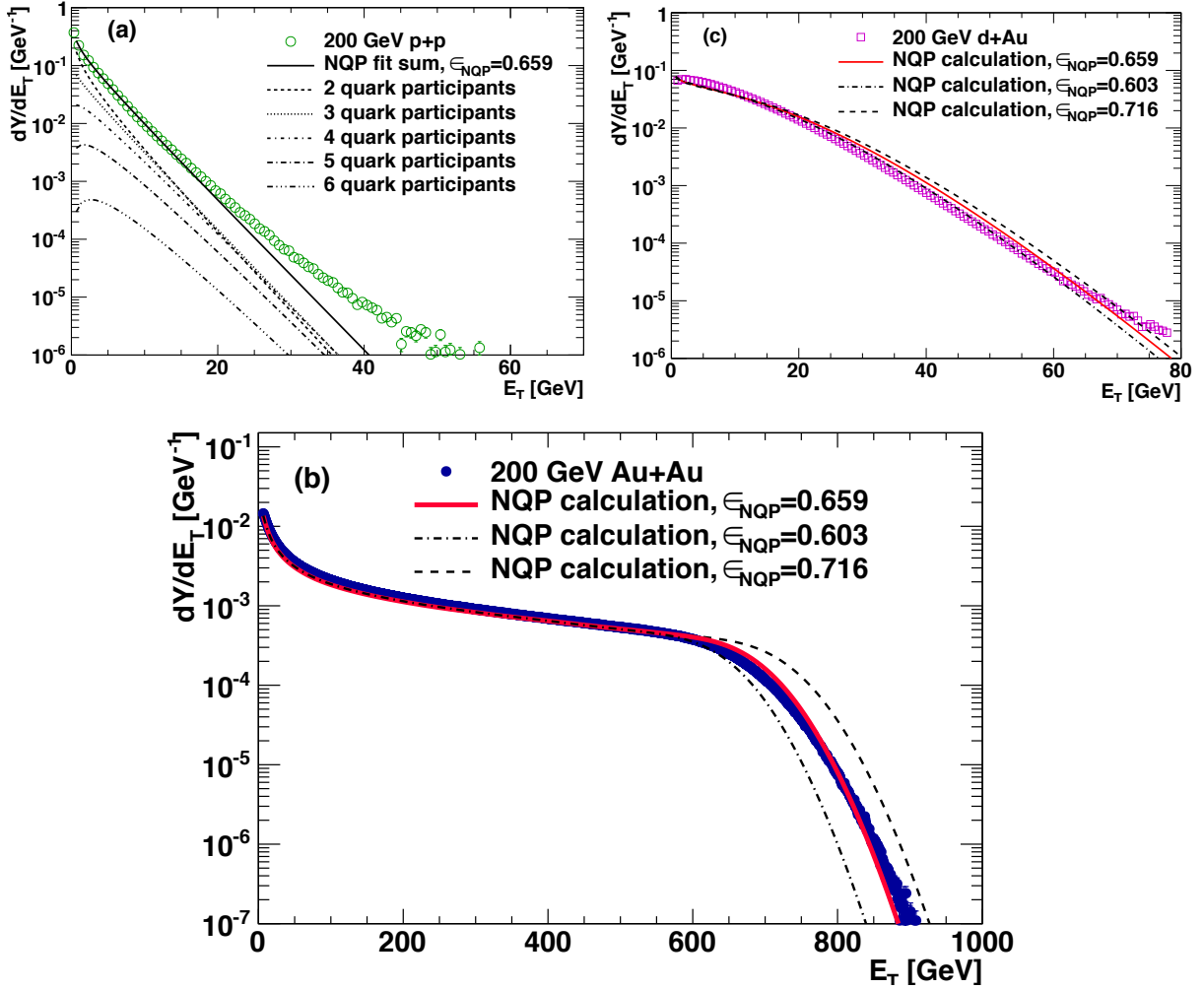


Figure 3: PHENIX2014⁸ method for $E_T \equiv dE_T/d\eta|_{y=0}$ distributions at $\sqrt{s_{NN}} = 200$ GeV: a) Deconvolution fit to the $p+p$ E_T distribution for $E_T < 13.3$ GeV for $\epsilon_{\text{NQP}} = 1 - p_{0\text{NQP}} = 0.659$ calculated in the Number of Quark Participants or N_{qp} model. Lines represent the properly weighted individual E_T distributions for the underlying 2,3,4,5,6 constituent quark participants plus the sum. b) Au+Au E_T distribution compared to the N_{qp} calculations using the central $1 - p_0 = 0.647$ and $\pm 1\sigma$ variations of $1 - p_0 = 0.582, 0.712$ for the probability p_0 of getting zero E_T on a $p+p$ collision with resulting quark participant efficiencies $\epsilon_{\text{NQP}} = 0.659, 0.603, 0.716$, respectively. (c) d+Au E_T distribution compared to the N_{qp} calculations as in (b).

where G_E and G_M are the electric and magnetic form factors of the proton, μ is its magnetic moment and Q^2 is the four-momentum-transfer-squared of the scattering. The inelastic $q+q$ cross section $\sigma_{q+q}^{\text{inel}} = 9.36$ mb at $\sqrt{s_{NN}} = 200$ GeV was derived from the $p+p$ N_{qp} Glauber calculation by requiring the calculated $p+p$ inelastic cross section to reproduce the measured $\sigma_{N+N}^{\text{inel}} = 42$ mb cross section, and then used for the Au+Au and d+Au calculations (Fig. 3).⁸

Sometimes people ask why we use Hofstadter's 60 year old measurements when there are more modern measurements which give a different proton r.m.s charge radius,²¹ which is not computed from Eq. 4 but merely from the slope of the form factor at $Q^2 = 0$. The answer is given in Fig. 4 which shows how all the measurements of $G_E(Q^2)$ and $G_M(Q^2)$ for

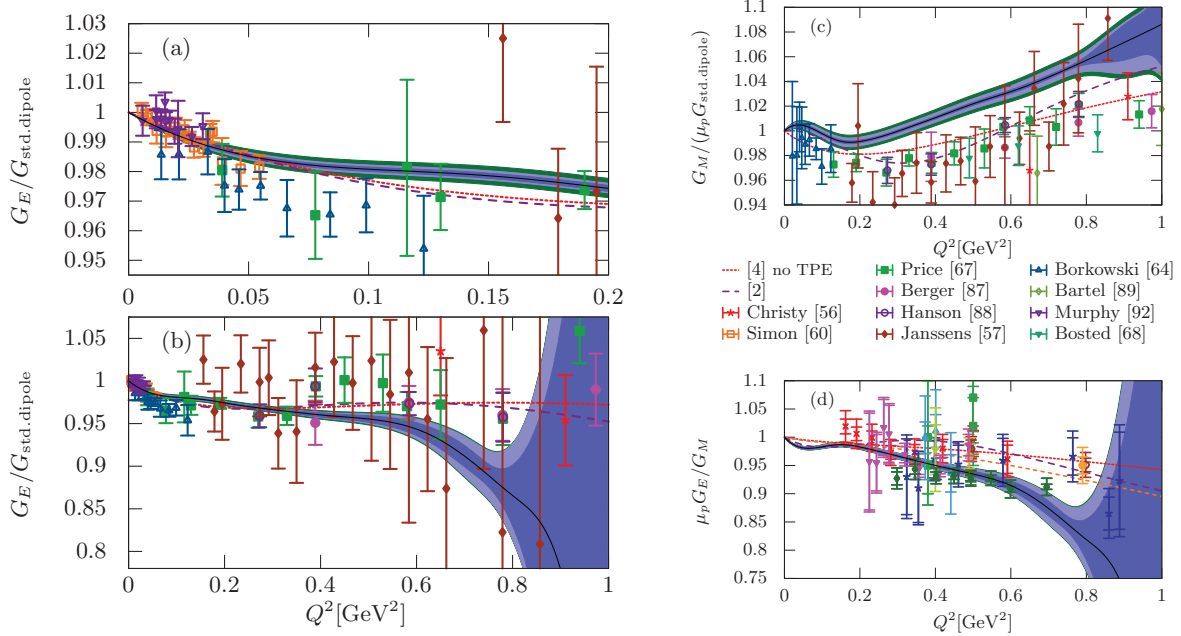


Figure 4: The form factors G_E and G_M , normalized to the standard dipole, and G_E/G_M , compared to fits, with the dark region being the best fit to the new Mainz data.²¹

$Q^2 \leq 1 \text{ GeV}^2$ agree with the “standard dipole” (Eq. 5) within a few percent, and in all cases in Fig. 4 agree as well if not better than the Mainz fit.

1.2 Improved method of generating constituent quarks

A few months after PHENIX2014 was published,⁸ it was pointed out to us that our method did not preserve the radial charge distribution (Eq. 3) about the c.m. of the three generated quarks. This statement is correct; so a few of us got together and found three new methods that preserve both the original proton c.m. and the correct charge distribution about this c.m.²² I discuss two of them here along with N_{qp} calculations using the PHENIX2014 data.⁸

1.2.1 Planar Polygon

Generate one quark at $(r, 0, 0)$ with r drawn from $r^2 e^{-4.27r}$. Then instead of generating $\cos \theta$ and ϕ at random and repeating for the two other quarks as was done by PHENIX2014,⁸ imagine that this quark lies on a ring of radius r from the origin and place the two other quarks on the ring at angles spaced by $2\pi/3$ radians. Then randomize the orientation of the 3-quark ring spherically symmetric about the origin. This guarantees that the radial density distribution is correct about the origin and the center of mass of the three quarks is at the origin but leaves the three-quark-triplet on each trial forming an equilateral triangle on the plane of the ring, which passes through the origin.

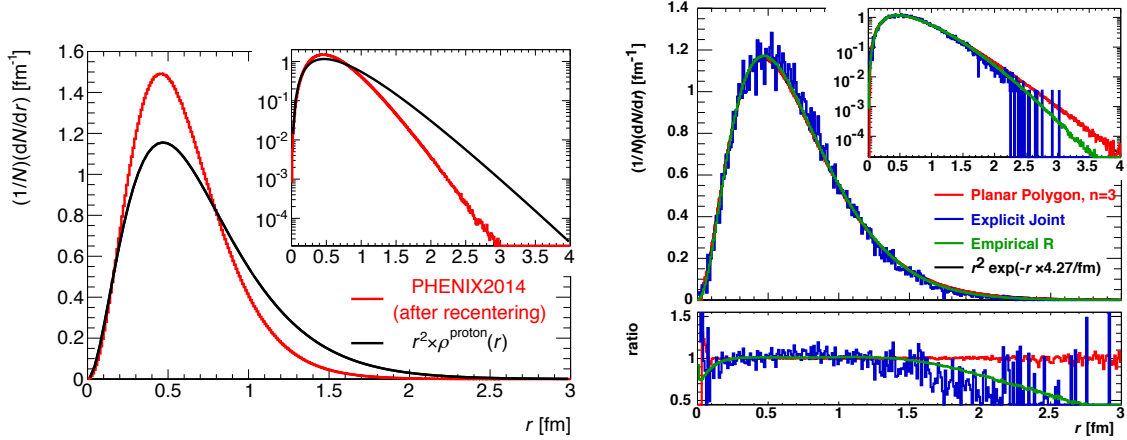


Figure 5: a) (left) Radial distribution dP/dr about the c.m. of the generated quark-triplets as a function of r [fm] for the PHENIX2014 method⁸ compared to $r^2\rho^{\text{proton}}(r)$ from Eq. 3 with semi-log plot as inset. b) (right) same for the 3 new methods and the ratios as indicated.²²

1.2.2 Empirical radial distribution, recentered

The three constituent quark positions are drawn independently from an auxiliary function $f(r)$:

$$f(r) = r^2\rho^{\text{proton}}(r) (1.21466 - 1.888r + 2.03r^2) (1 + 1.0/r - 0.03/r^2) (1 + 0.15r) . \quad (6)$$

Then the center of mass of the generated three-quark system is re-centered to the original nucleon position. This function was derived through an iterative, empirical approach. For a given test function $f^{\text{test}}(r)$, the resulting radial distribution $\rho^{\text{test}}(r)$ was compared to the desired distribution $\rho^{\text{proton}}(r)$ in Eq. 3. The ratio of $\rho^{\text{test}}(r)/\rho^{\text{proton}}(r)$ was parameterized with a polynomial function of r or $1/r$, and the test function was updated by multiplying it with this parametrization of the ratio. Then, the procedure was repeated with the updated test function $f^{\text{test}}(r)$ used to generate an updated $\rho^{\text{test}}(r)$ until the ratio $\rho^{\text{test}}(r)/\rho^{\text{proton}}(r)$ was sufficiently close to unity over a wide range of r values. Figure 5 shows²² the generated radial distributions compared to $r^2\rho^{\text{proton}}(r)$ from Eq.3.

1.3 New N_{qp} results using PHENIX2014 data

From Fig. 5b, the Planar Polygon method is identical to Eq. 3 but has all three quarks at the same radius from the c.m. of the proton, which can be tested with more information about constituent quark correlations in a nucleon. The Empirical Recentered method follows $r^2\rho^{\text{proton}}(r)$ well out to nearly $r = 2$ fm, $Q^2 = 0.25 \text{ fm}^{-2} = 0.01 \text{ GeV}^2$ (compare Fig. 4a,b), and is now adopted as the standard.²³ The results of the N_{qp} calculations with the Empirical Recentered method²² for the PHENIX2014 data (Fig. 6), are in excellent agreement with the d+Au data and agree with the Au+Au measurement to within 1σ of the calculation (7% higher in E_T). The PHENIX2014 calculation (Fig. 3b) is only 1.2σ in E_T below the new calculation so that the PHENIX2014 N_{qp} results and conclusions⁸ are consistent with the new standard method.²²

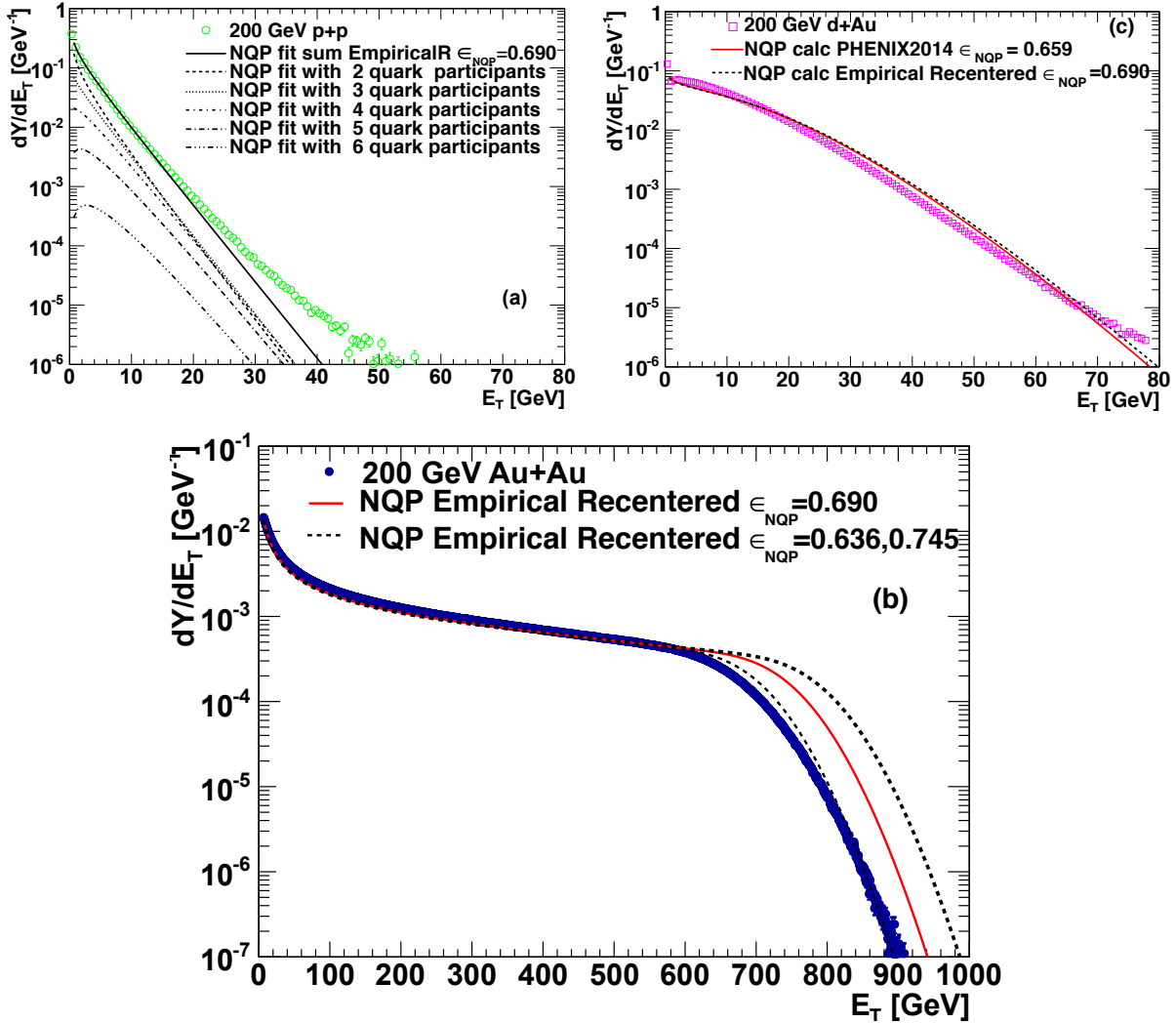


Figure 6: New N_{qp} results²² for $E_T \equiv dE_T/d\eta|_{y=0}$ distributions at $\sqrt{s_{NN}} = 200$ GeV using and compared to PHENIX2014⁸ data. a) p+p, b) Au+Au, c) d+Au.

2 Constituent quark participant scaling vs. centrality for Multiplicity and E_T distributions

In Fig. 7,²⁴ the linear dependence of $dE_T/d\eta$ and $dN_{ch}/d\eta$ on the number of constituent quark participants N_{qp} is demonstrated by the constant values of $(dE_T/d\eta)/(0.5N_{qp})$ and $(dN_{ch}/d\eta)/(0.5N_{qp})$ with centrality represented as N_{qp} . The N_{qp} calculations are made with the now standard Empirical Recentered method.²² The relevant issue for the present discussion is to notice the $\pm 1\sigma$ correlated systematic errors indicated by the dashes. For instance, in Fig. 7b all the data points for 200 GeV Au+Au can be moved up by $+1\sigma$ of the correlated systematic error to the dashed line at the cost of only $1.0^2 = +1.0$ to the value of χ^2 of a fit with all 10 points moved. In detail this means that the lowest $(dN_{ch}/d\eta)/(0.5N_{qp}) = 1.35 \pm 0.20$ data point at $N_{qp} = 78$ can be moved up to the dashed line as 1.50 ± 0.22 and all the other data points will move up to the dashed line.

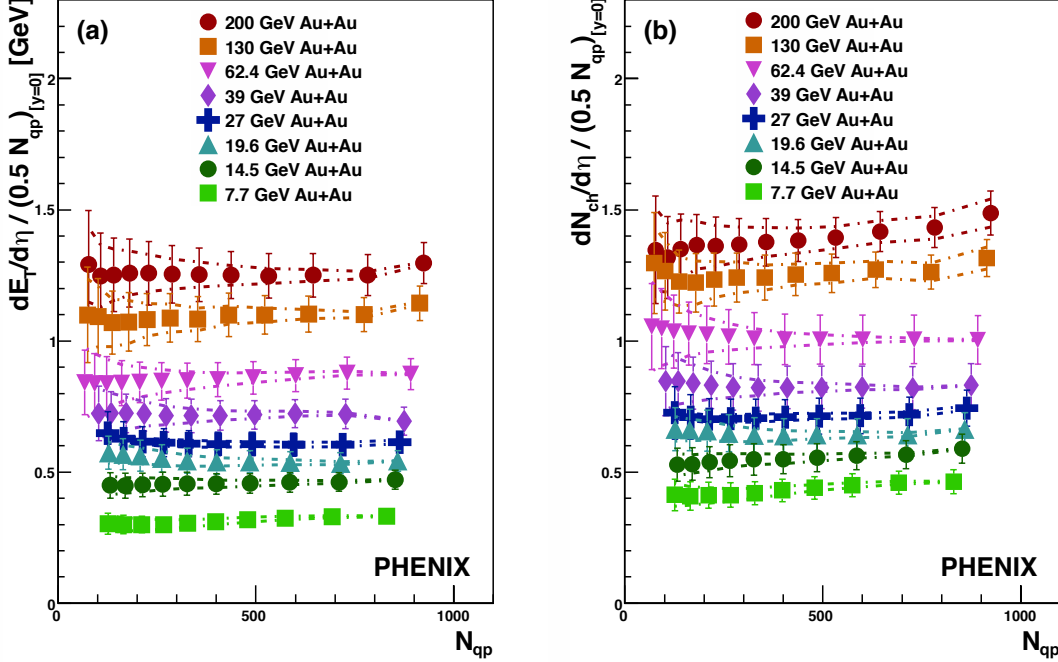


Figure 7: (a) $(dE_T/d\eta)/(0.5N_{qp})$ and (b) $(dN_{ch}/d\eta)/(0.5N_{qp})$ at midrapidity as a function of N_{qp} for Au+Au collisions at $\sqrt{s_{NN}}=200, 130, 62.4, 39, 27, 19.6, 14.5,$ and 7.7 GeV. *The lines bounding the points represent the trigger efficiency uncertainty within which the points can be tilted.* The error bars represent the remaining total statistical and systematic uncertainty.²⁴

2.1 Disagreement from another N_{qp} calculation?

Bozek, Broniowski and Rybczynski²⁵ did a calculation for constituent quark participants, which they call Q_W (wounded quark) and for N_{part} they use N_W (Fig. 8a). They find that the N_{qp} scaling works for Alice Pb+Pb at $\sqrt{s_{NN}}=2.76$ TeV but they make the comment “we note in Fig. 1 (Fig. 8a here) that at $\sqrt{s_{NN}}=200$ GeV the corresponding p+p point is higher by about 30% from the band of other reactions.” However, there are several things to note in Fig. 8a that Bozek *et al.* seem to have missed.

Figure 8b shows that the 30% is only valid for the lowest Au+Au and the d+Au points. The second thing to note is that they only used the tabulated data points²⁴ which did not include the correlated systematic errors which were indicated by dashes on the figures (see the italicized sentence in the caption of Fig. 7 which admittedly is not as clear as it could be). If all the data points are moved up to the top of their $+1\sigma$ correlated systematic error (dashed line in Fig. 7b, with a cost of 1σ (Fig. 8c)), then the ratio of the p+p to the lowest Au+Au point is 1.19 ± 0.17 , i.e. statistical 1.1σ , plus the systematic $+1\sigma$ in quadrature, which equals a 1.5σ difference which is not significant. Regarding, the lowest d+Au (and $^3\text{He}+\text{Au}$) data points which were mentioned²⁵ in the discussion of Fig. 8a, they are shown on a better scale without their correlated systematic error in Fig. 9a and are in agreement with the lowest Au+Au data points.

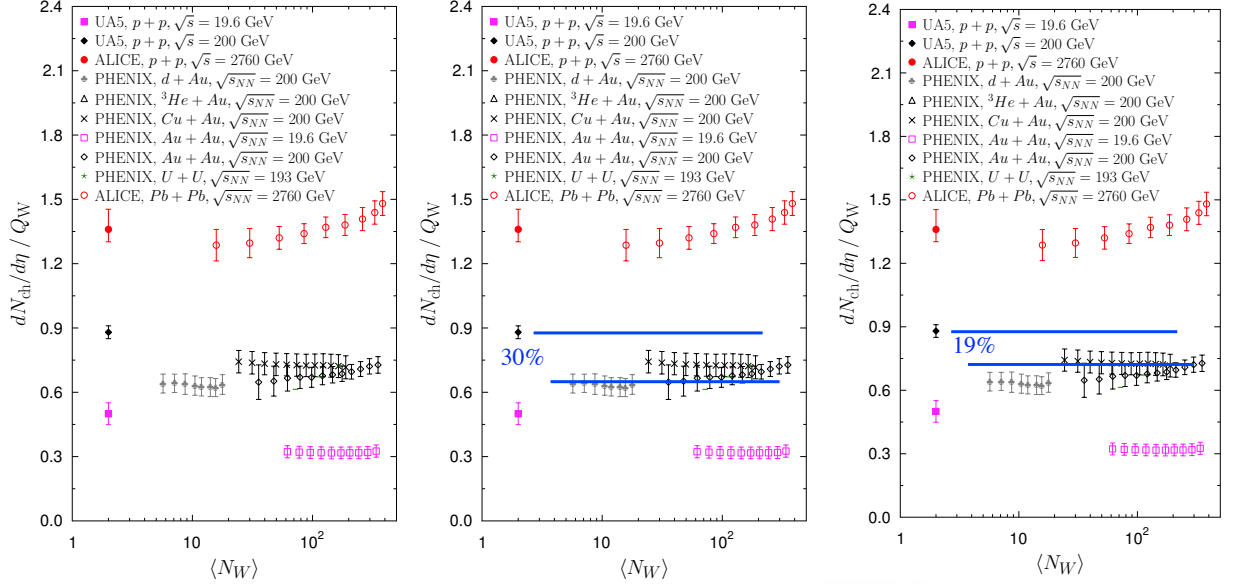


Figure 8: a) (left) Experimental multiplicity of charged hadrons per unit of pseudorapidity (at midrapidity) divided by the number of wounded quarks, $dN_{\text{ch}}/d\eta/Q_W$, plotted as a function of centrality expressed via the number of wounded nucleons N_W .²⁵ b) (center) Same as (a) with 30% difference from the lowest Au+Au measured data point to the p+p calculated data point indicated. c) (left) Same as (b) except 19% difference from the top of the Au+Au $+1\sigma$ correlated systematic error.

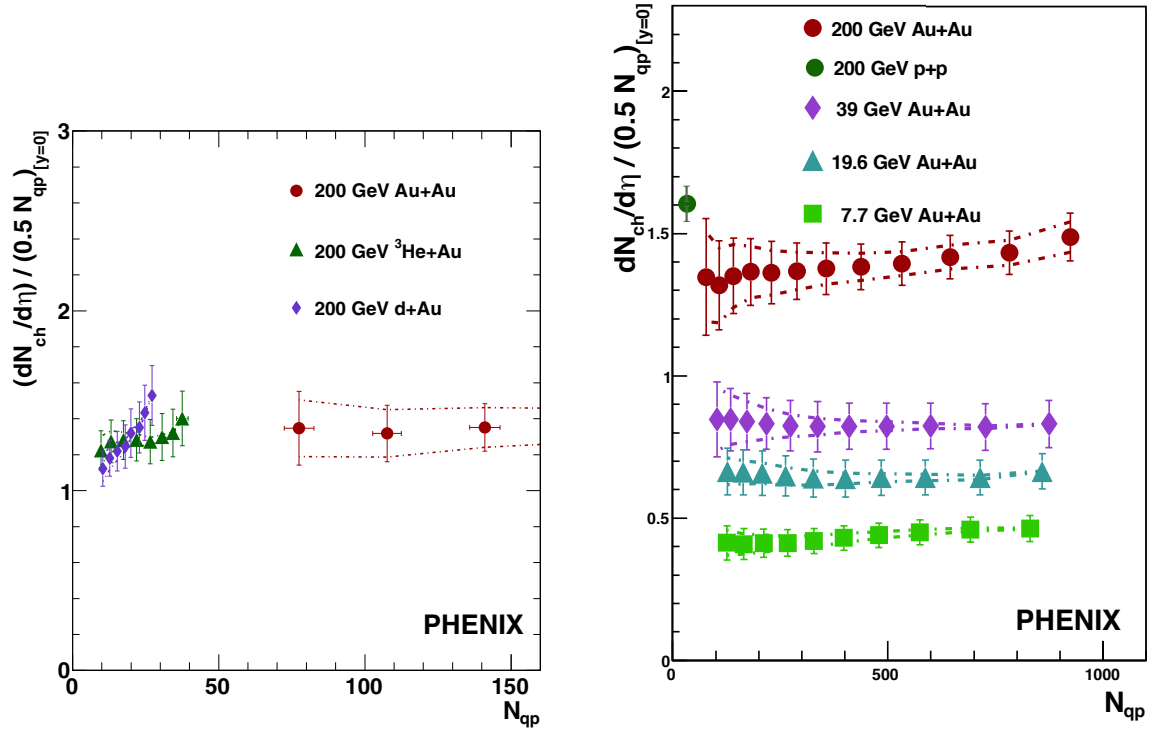


Figure 9: a) (left) $(dN_{\text{ch}}/d\eta)/(0.5N_{qp})$ as a function²⁴ of N_{qp} for d+Au, $^3\text{He}+\text{Au}$ at $\sqrt{s_{NN}}=200$ GeV compared to the least central of the Au+Au data. b) (right) $(dN_{\text{ch}}/d\eta)/(0.5N_{qp})$ for $\sqrt{s_{NN}}=200, 39, 19.6$ and 7.7 GeV Au+Au data of Fig. 7, with the p+p calculated data point added.

2.2 Something that we left out.

Although the correlated systematic errors were shown on Fig. 7 for the Au+Au results, we actually did not calculate the p+p value of $(dN_{\text{ch}}/d\eta)/(0.5N_{\text{qp}})$ when we wrote the paper.²⁴ To compare with Bozek *et al.*,²⁵ I used the same UA5 $\bar{\text{p}}+\text{p}$ $dN_{\text{ch}}/d\eta = 2.23 \pm 0.08$ at $\sqrt{s} = 200$ GeV²⁶ that they used together with the PHENIX2014 value²⁴ of $\langle N_{\text{qp}} \rangle = 2.78$ for p+p collisions, with the result $(dN_{\text{ch}}/d\eta)/(0.5N_{\text{qp}})_{\text{pp}} = 1.60 \pm 0.06$ shown on Fig. 9b. This is in agreement to within $\approx 1\sigma$ with all the Au+Au $\sqrt{s} = 200$ data points in Fig. 9b. It is important to note that if the $dN_{\text{ch}}/d\eta$ in p+p collisions had been measured by PHENIX in Figs. 8 and 9 then only the statistical errors σ could be used for comparison because all the data points (including the p+p data) would move together by their common correlated systematic error. However, since the p+p $dN_{\text{ch}}/d\eta$ measurement is from a different experiment²⁶ the PHENIX A+A measurements and correlated systematic errors are independent of the p+p measurement as assumed in section 2.1.

Table 1: Table N_{qp} in p+p

	paper	$\sqrt{s_{NN}}$	$\sigma_{nn}^{\text{inel}}$	r_m	$\sigma_{qq}^{\text{inel}}$	$\langle N_{\text{qp}} \rangle$
	p+p	(GeV)	(mb)	(fm)	(mb)	
PX2014 Phys. Rev. C	89 , 044905 (2014)	200	42.0	0.81	9.36	2.99
MPTS Phys. Rev. C	93 , 054910 (2016)	200	42.3	0.81	8.17	2.78
Loizides Phys. Rev. C	94 , 024914 (2016)	200	42.	0.81	8.1	2.8
BB&R Phys. Rev. C	94 , 014902 (2016)	200	41.3	0.94	7.0	2.60

reaction	dn/deta	err	sys	QW	err	
p+p Bozek	2.29	0.08		2.6		
p+pMJTBozek	2.23	0.08		2.6		
p+p MPTS	2.23	0.08		2.78		
cent 55-60				QW	err	
AuAu Bozek	52.2	6.5	4.88	80.65		
AuAuPX	52.2	6.5	4.88	77.5	6.8	
	dnch/QW	err				
p+p Bozek	0.881	0.031				
p+pMJTBozek	0.858	0.031				
p+p MPTS	0.802	0.029				
	dnch/QW	stat	sys			
AuAu Bozek	0.647	0.081	0.061			
AuAuPX	0.674	0.103	0.086			
		stat	sys	stat+sys	shift sys	stat
pp/Au Bozek	1.361	0.176	0.136	0.222	1.225	0.176
ppmjtB/AuB	1.325	0.172	0.133	0.217	1.192	0.172
pp/AuAu PX	1.191	0.186	0.159	0.245	1.032	0.186

Figure 10: (top) Table 1, N_{qp} calculations in p+p collisions by four different publications indicated. (bottom) More details of the calculations in Table 1 where Bozek refers to BB&R,²⁵ PX refers to PHENIX2014⁸ and MJTBozek refers to the p+p calculation in Fig. 9b.

2.2.1 Why are the Bozek *et al.*²⁵ (BB&R) results different from the PHENIX calculation?

The calculation of $\langle N_{qp} \rangle$ for p+p collisions seems to be the culprit. Table 1 gives values for four independent calculations in p+p collisions. As far as I can tell BB&R²⁵ used $r_m = 0.94$ fm for the proton rms radius in Eq. 3 instead of $r_m = 0.81$ fm. They also used a “Gaussian wounding profile” for a q+q collision which is not the standard Glauber Monte Carlo method. The tables in Fig. 10 give more details about the various constituent quark calculations for $\sqrt{s_{NN}} = 200$ GeV.

3 Conclusions

- i) The constituent quark participant model (N_{qp}) works at mid-rapidity for A+B collisions in the range (~ 20 GeV) $39 \text{ GeV} \leq \sqrt{s_{NN}} \leq 5.02 \text{ TeV}$.
- ii) Experiments generally all use the same Glauber Monte Carlo method but the BB&R²⁵ Monte Carlo is different for q+q scattering leading to somewhat different results.
- iii) Attention must be paid to correlated systematic errors.
- iv) How can the event-by-event proton radius variations and quark-quark correlations used in constituent quark Glauber calculations be measured?

References

- [1] W. Busza, et al., *Phys. Rev. Lett.* **34**, 836–839 (1975).
- [2] See also M. J. Tannenbaum, *Int. J. Mod. Phys. A* **4**, 3377–3476 (1989) and *Mod. Phys. Lett. A* **9**, 89–100 (1994).
- [3] A. Bialas, M. Bleszynski and W. Czyz, *Nucl. Phys. B* **111**, 461–476 (1976).
- [4] PHENIX Collaboration, K. Adcox, *et al.*, *Phys. Rev. Lett.* **86**, 3500–3505 (2001).
- [5] PHENIX Collaboration, K. Adcox, *et al.*, *Phys. Rev. Lett.* **87**, 052301 (2001).
- [6] WA98 Collaboration, M.M. Aggarwal, *et al.*, *Eur. Phys. J. C* **18**, 651–663 (2001).
- [7] PHENIX Collaboration, A. Adare, *et al.*, *Phys. Rev. C* **77**, 064907 (2008).
- [8] PHENIX Collaboration, S. S. Adler, *et al.*, *Phys. Rev. C* **89**, 044905 (2014).
- [9] M. Gell-Mann, *Phys. Lett.* **8**, 214–215 (1964).
- [10] A. H. Mueller, *Nucl. Phys. A* **527**, 137c–152c (1991).
- [11] G. Morpurgo, *Ann. Rev. Nucl. Part. Sci.* **20**, 105–146 (1970).

- [12] E. V. Shuryak, *Nucl. Phys. B* **203**, 116–139 (1982).
- [13] MIT-SLAC Collaboration, M. Breidenbach, *et al.*, *Phys. Rev. Lett.* **23**, 935–939 (1969).
- [14] PHENIX Collaboration, A. Adare, *et al.*, *Phys. Rev. D* **76**, 051106(R) (2007).
- [15] S. Eremin and S. Voloshin, *Phys. Rev. C* **67**, 064905 (2003).
- [16] R. Nouicer, *Eur. Phys. J. C* **49**, 281–286 (2007).
- [17] B. De and S. Bhattacharyya, *Phys. Rev. C* **71**, 024903 (2005).
- [18] R. Hofstadter, *Rev. Mod. Phys.* **28**, 214–254 (1956).
- [19] R. Hofstadter, F. Bumiller, and M. R. Yerian, *Rev. Mod. Phys.* **30**, 482–497 (1958).
- [20] L. N. Hand, D. G. Miller, and R. Wilson, *Rev. Mod. Phys.* **35**, 335–349 (1963).
- [21] A1 Collaboration, J. C. Bernauer *et al.*, *Phys. Rev. C* **90**, 015206 (2014).
- [22] J. T. Mitchell, D. V. Perepelitsa, M. J. Tannenbaum, and P. W. Stankus, *Phys. Rev. C* **93**, 054910 (2016).
- [23] C. Loizides, *Phys. Rev. C* **94**, 024914 (2016).
- [24] PHENIX Collaboration, A. Adare, *et al.*, *Phys. Rev. C* **93**, 024901 (2016).
- [25] P. Bozek, W. Broniowski, and M. Rybczynski, *Phys. Rev. C* **94**, 014902 (2016).
- [26] UA5 Collaboration, G. J. Alner, *et al.*, *Z. Phys. C* **33**, 1–6 (1986).